ЖЭТФ, 2011, том 139, вып. 1, стр. 119–125

GRAPHENE-BASED MODULATION-DOPED SUPERLATTICE STRUCTURES

D. Bolmatov*[*], *Chung-Yu Mou

Department of Physics, National Tsing Hua University, Hsinchu 300, Taiwan

National Center for Theoretical Sciences, Hsinchu 300, Taiwan

Department of Physics, Queen Mary University of London
E 1 4NS, London, UK

Received July 8, 2010

The electronic transport properties of graphene-based superlattice structures are investigated. A graphene-based modulation-doped superlattice structure geometry is proposed consisting of periodically arranged alternate layers: InAs/graphene/GaAs/graphene/GaSb. The undoped graphene/GaAs/graphene structure displays a relatively high conductance and enhanced mobilities at increased temperatures unlike the modulation-doped superlattice structure, which is more steady and less sensitive to temperature and the robust electrical tunable control on the screening length scale. The thermionic current density exhibits enhanced behavior due to the presence of metallic (graphene) monolayers in the superlattice structure. The proposed superlattice structure might be of great use for new types of wide-band energy gap quantum devices.

1. INTRODUCTION

Graphene — a single layer of carbon atoms densely packed in a honeycomb structure — was recently first isolated in its free-standing form [1, 2]. However, its unusual material and physical properties have already captured the interest of many researchers working in condensed-matter physics [3–6]. This two-dimensional material has a very high quality, is extremely strong, it exhibits ballistic electronic transport on the micrometer scale at room temperature, and can be chemically doped, and its conductivity can be controlled with an electric field [7–10]. Graphene has a linear gapless spectrum, and therefore exhibits metallic conductivity even in the limit of a nominally zero carrier concentration [11–13]. At the same time, most electronic applications rely on the presence of a gap between the valence and conduction bands [14–19].

The continuing enhancing of quantum electronic devices poses new challenges to the semiconductor industry for each new device generation [20–22]. At the mesoscopic scale, there are important quantum effects, and the materials that worked well in previous-generation devices do not perform properly at the nanoscale, and hence new materials need to be introduced [23]. Eventually, not only the materials [24] but also the basic device operation principles and geometries need to be revised [25].

Superlattices have been used to filter the energy of electrons [26, 27]. The band structure can be tuned by varying the composition and thickness of the layers [28]. In fact, superlattices are widely used in applications that have nothing to do with their electronic properties [29–31]. This is to improve the cleanliness of material during growth [32]. The structures discussed below are vertical, in the sense that the current flows along the direction of growth or along the normal to the interface [33]. The obvious way of introducing carriers, used in classical devices, is to dope the regions where electrons or holes are desired [34, 35]. The solution is the remote or modulation doping, where the doping increases in one region, but the carriers subsequently migrate to another [36]. Modulation doping has achieved two benefits: it has separated electrons from their donors (holes from their acceptors) to reduce scattering by ionized impurities, and the electrons (holes) to two dimensions.

In this paper, we propose a new graphene-based modulation-doped superlattice structure geometry

[*]E-mail: bolmat@phys.nthu.edu.tw

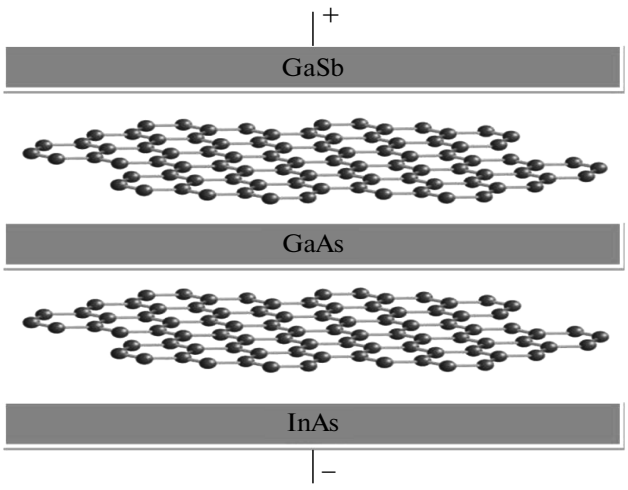

Fig. 1. Tunneling structure of the graphene device. Two monolayers of graphene are sandwiched between thin layers of InAs at the bottom of the quantum device and thin layers of GaSb at the top. GaAs is placed in the middle

that consist of periodically arranged alternate layers: InAs/graphene/GaAs/graphene/GaSb. Figure 1 illustrates the graphene device tunneling structure: monolayers of graphene are sandwiched between thin layers of InAs at the bottom of the quantum device and thin layers of GaSb at the top. In the middle of the proposed superlattice structure, gallium arsenide (GaAs) is placed, which has a higher saturated electron velocity and higher electron mobility and has some electronic properties that are superior to those of silicon. GaAs devices are relatively insensitive to heat and generate less noise than silicon devices when operated at high frequencies. GaAs layer is captured by two graphene monolayers. Weak anti-localization, mobility, and carrier density of the graphene allow considering this geometry as an *intrinsic* semiconductor structure, which we treat in the first section of our work. The weak van der Waals forces that provide the cohesion of multilayer graphene stacks do not always affect the electronic properties of the individual graphene layers in the stack.

Our idea here is to create two high-conductivity channels in the current-spreading graphene layers, one of which is sandwiched by GaAs (gapped material) at the top and by InAs (electrons-doped region) at the bottom, and the other is sandwiched by GaAs (gapped material) at the bottom and by GaSb (holes-doped region) at the top. Electronic transport properties of this structure are investigated in Sec. 2.

2. ELECTRONIC PROPERTIES

Pure semiconductors that are free from impurities are called *intrinsic* semiconductors. Ideally, the intrinsic conductivity is zero at 0 K and increases with temperature owing to the thermal excitation of electrons from the valence to the conduction band. The electrons thus excited leave holes in the valence band. The electric conductivity in these materials is due to both the electrons in the conduction band and the holes in the valence band. The conductivity in these materials can be written as

$$\sigma = n_e e \mu_e + n_h e \mu_h, \tag{1}$$

where n_e and n_h are the electron and hole concentrations, μ_e and μ_h are the electron and hole mobilities (200000 $\mathrm{cm}^2/\mathrm{V}\cdot\mathrm{s}$ in graphene, 3000000 $\mathrm{cm}^2/\mathrm{V}\cdot\mathrm{s}$ in two-dimensional electron gases), and e the charge of the electron or the hole. The number of electrons available in the conduction band depends on two factors: the number of electronic energy levels available in the conduction band and the extent to which these energy states are occupied. The first is given by the density of states and the second factor comes from the Fermi–Dirac distribution function.

If $f(E)$ is the probability of finding the electron in the energy state with energy E, then $1 - f(E)$ is the probability for the electron (or the hole) to not be found in that state. The total number N of electrons is given by

$$N = \sum_i \frac{1}{\exp(\beta(E_i - \mu)) + 1} + \\ + \sum_j \frac{1}{\exp(\beta(E_j - \mu)) + 1}, \tag{2}$$

where E_i is an energy level in the conduction band and E_j is an energy level in the filled band. In the case of an intrinsic semiconductor, the total number of electron states in the filled band is equal to N, that is,

$$\sum_j 1 = N.$$

Hence, it follows from Eq. (2) that

$$\sum_i \frac{1}{\exp(\beta(E_i - \mu)) + 1} = \\ = \sum_j \left(1 - \frac{1}{\exp(\beta(E_j - \mu)) + 1}\right) = \\ = \sum_j \frac{1}{\exp(\beta(-E_i + \mu)) + 1}. \tag{3}$$

This shows the equality of the number of conduction electrons (the left-hand side) and number of holes in the filled band (the right-hand side) in intrinsic semiconductors,

$$n_e = n_h. \tag{4}$$

The number of electrons in the conduction band (the number of holes in the valence band) is obtained by integrating the expression

$$n_e = \int_{E_g}^{\infty} D(E)f(E)\,dE, \quad n_h = \int_{-\infty}^{0} D(E)(1-f(E))\,dE.$$

Here, the origin of energy is taken at the top of the filled band and the inequality $E_g \gg kT$ is assumed. Substituting the expressions for $D(E)$ and $f(E)$, we then have

$$n_e = \frac{1}{\pi}\int_{E_g}^{\infty} \frac{E-E_g}{(\hbar v_F^e)^2} \exp\left[\frac{\mu - E}{kT}\right] dE \tag{5}$$

for electrons and

$$n_h = \frac{1}{\pi}\int_{-\infty}^{0} \frac{(-E)}{(\hbar v_F^h)^2} \exp\left[\frac{-\mu + E}{kT}\right] dE \tag{6}$$

for holes. Now the electron and hole densities become

$$n_e = \frac{1}{\pi}\left(\frac{kT}{\hbar v_F^e}\right)^2 \exp\left[\frac{\mu - E_g}{kT}\right], \tag{7}$$

$$n_h = \frac{1}{\pi}\left(\frac{kT}{\hbar v_F^h}\right)^2 \exp\left[-\frac{\mu}{kT}\right]. \tag{8}$$

From equations (7), (8), and (4), we can determine $\exp(\mu/kT)$ as

$$\exp\left(\frac{\mu}{kT}\right) = \frac{v_F^e}{v_F^h}\exp\left(\frac{E_g}{2kT}\right). \tag{9}$$

It therefore follows from (7) and (8) that

$$n_e = n_h = \frac{1}{\pi v_F^e v_F^h}\left(\frac{kT}{\hbar}\right)^2 \exp\left(-\frac{E_g}{2kT}\right). \tag{10}$$

Equation (9) yields

$$\mu = \frac{1}{2}E_g + kT\log\frac{v_F^e}{v_F^h}. \tag{11}$$

The chemical potential μ in (11) lies in the vicinity of the middle of the forbidden energy gap if the value of $\log(v_F^e/v_F^h)$ (where $v_F^e \approx 1.11\cdot 10^6$ m/s, $v_F^h \approx 1.04\cdot 10^6$ m/s in graphene monolayer and $v_F^e \approx 1.10\cdot 10^6$ m/s, $v_F^h \approx 1.07\cdot 10^6$ m/s in layered graphene) is of the order of unity and the temperature is well below E_g/k. Hence, the relations $E_g/k \gg T$, $E_g - \mu \gg kT$ and $\mu \gg kT$ are satisfied at ordinary temperature.

3. MODULATION-DOPED SUPERLATTICES

3.1. Neutrality

Because semiconductors contain mobile electric charges, they tend to be electrically neutral, which is to say they contain equal amounts of positive and negative charge. It is interesting to see how large a non-neutral region can be, without the occurrence of large potential differences.

We focus on graphene-based modulation-doped superlattice structures. Inherently, InAs and GaSb are doping layers in a superlattice structure; graphene monolayers make the electric carriers highly mobile and the GaAs layer is active. We propose a varying potential that tends to a constant value, taken as zero. In the constant potential, the hole (electron) density n_0 is equal to the acceptor (donor) density A (without losing the generality, we consider the p-type (hole) carriers). Where the potential has charged to V, the hole density is controlled by the Maxwell–Boltzmann relation

$$n = n_0 \exp\left(-\frac{eV}{kT}\right)$$

(we recall assumption $E_g \gg kT$). In this case, the Poisson equation is

$$\frac{d^2V}{dx^2} = \frac{-e}{\epsilon_s\epsilon_0}(n - A) = \\ = \frac{-\epsilon n_0}{\epsilon_s\epsilon_0}\left(\exp\left(-\frac{eV}{kT}\right) - 1\right), \tag{12}$$

where ϵ_0 is the permittivity and ϵ_s is the relative permittivity of the active region.

This equation is unpleasant to solve in the general case, but when $|eV/kT| \ll 1$, we can use the first two terms in a series approximation for the exponential, which gives

$$\frac{d^2V}{dx^2} = \frac{e^2 n_0}{\epsilon_s\epsilon_0 kT}V. \tag{13}$$

Equation (13) has a solution

$$V = V_0 \exp\left(-x/\lambda_D\right), \tag{14}$$

where

$$\lambda_D = \sqrt{\frac{kT\epsilon_s\epsilon_0}{e^2 n_0}}$$

is the Debye length. Equation (13) shows that a perturbation in the potential tends to increase or decrease over distances of the order of λ_D.

Major field changes occur over distances longer than λ_D. In what follows, we consider a superlattice structure with different boundary conditions, taking into account that graphene is quite different from most conventional three-dimensional materials: intrinsic graphene is a semimetal or zero-gap semiconductor. We set $x = 0$ at the surface of the lower graphene monolayer and assume the potential to be zero at $x = 0$. The electron gas outside the metal is so rarefied that it can be treated classically. Then $V(x)$ increases as x increases from 0 to infinity, and $V(\infty) = \infty$ because $n(\infty) = 0$, and $V'(\infty) = 0$ because the electric field should vanish as $x \to \infty$. In terms of V, the Poisson equation can be written as

$$V'' = -\frac{e^2 n_0}{\epsilon_s\epsilon_0} \exp\left(-\frac{eV}{kT}\right). \tag{15}$$

Multiplying this by V' and integrating, and using the boundary conditions given above, we obtain

$$\frac{1}{2}(V')^2 = \frac{n_0 e^2}{\epsilon_s\epsilon_0} kT \exp\left(-\frac{eV}{kT}\right), \tag{16}$$

whence

$$V' = \left(\frac{2n_0 e^2}{\epsilon_s\epsilon_0} kT\right)^{\frac{1}{2}} \exp\left(-\frac{eV}{2kT}\right). \tag{17}$$

Integrating this result once again yields

$$\exp\left(\frac{eV}{kT}\right) = \left(\frac{2n_0 e^2}{\epsilon_s\epsilon_0 kT}\right)^{1/2} (x + \lambda_D). \tag{18}$$

Because we have assumed that $V(0) = 0$, substituting $x = 0$ in (18) yields the value of the integration constant λ_D. Therefore, (18) can be rewritten as

$$\exp\left(\frac{eV}{kT}\right) = \frac{x}{\lambda_D} + 1,$$

whence

$$V = 2V_0 \log\left(\frac{x + \lambda_D}{\lambda_D}\right). \tag{19}$$

Substituting this in (12), we finally obtain

$$n(x) = n_0 \left(\frac{\lambda_D}{x + \lambda_D}\right)^2. \tag{20}$$

Electrical potential behavior is illustrated in Fig. 2.

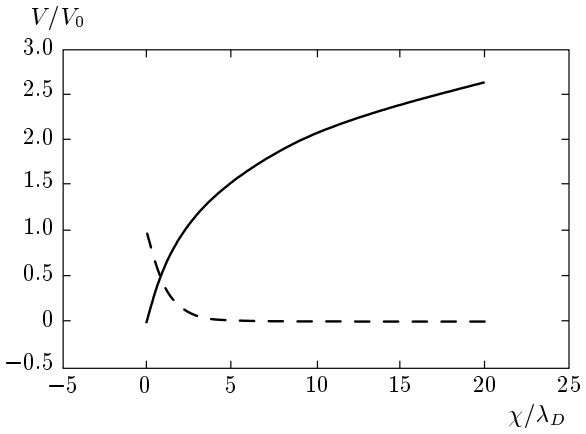

Fig. 2. Electrostatic potential behavior in term of screening length units. The dashed line (V_1) is calculated from (14) and the solid line (V_2) is calculated from (19)

3.2. Boltzmann transport equation

In the preceding section, we considered the case of intrinsic semiconductors, where the number of electrons that are excited to the conduction band is equal to the number of holes in the valence band. The electric conductivity of electrons or holes in graphene-based superlattice structures due to the doping electrons (confined to one material, InAs) and holes (confined to the other, GaSb) can be investigated by considering the Boltzmann transport equation

$$\frac{\partial f}{\partial t} + \mathbf{v} \cdot \frac{\partial f}{\partial \mathbf{x}} + \mathbf{F} \cdot \frac{\partial f}{\partial \mathbf{k}} = \left(\frac{\partial f}{\partial t}\right)_{coll}, \tag{21}$$

where $\mathbf{x}$ is the coordinate, $\mathbf{k}$ the momentum, f the distribution function of carriers, and $\mathbf{F}$ the external force acting on a particle. In the paradigm of graphene-based modulation-doped superlattice structures of InAs/graphene/GaAs/graphene/GaSb, the interface modes in graphene monolayers emerge as crucial factors and the higher-frequency mode produces a symmetric field in the GaAs well, which markedly enhances the intrasubband scattering rate.

It suffices to find the current density in the form of a term proportional to the electric field. Under the assumptions of steadiness and uniformity, the Boltzmann equation becomes

$$-e\mathbf{E} \cdot \frac{\partial f}{\partial \mathbf{k}} = -\frac{f - f_0}{\tau}. \tag{22}$$

In order to determine an expression correct to the first order in $\mathbf{E}$, the distribution function f in the right-hand side may be replaced by the zeroth approximation f_0,

i. e., the solution in the case where $\mathbf{E} = 0$. Noting that f_0 is a function of E, we obtain

$$f = f_0 + \frac{\partial f_0}{\partial E}\tau e\mathbf{v}\cdot\mathbf{E}. \tag{23}$$

According to this expression, the electric current is produced by a shift of the center of the Fermi distribution. This is most clearly seen in the case where $\varepsilon(\mathbf{k}) = \hbar v\mathbf{k}$:

$$f \coloneqq f_0(\varepsilon + \tau e\mathbf{v}\cdot\mathbf{E}).$$

The current density is obtained by multiplying Eq. (23) by $-ev$ and integrating over all values of the momentum,

$$\mathbf{j} = -e\int v f\frac{4d\mathbf{k}}{h^2} = e^2\int\left(-\frac{\partial f_0}{\partial\varepsilon}\right)\tau v\mathbf{v}\cdot\mathbf{E}\frac{4d\mathbf{k}}{h^2}, \tag{24}$$

where $d\mathbf{k}$ stands for $dk_x\cdot dk_y$ and the factor 4 accounts for the weight due to spin and valley. Therefore, the components of the electric conductance can be written as

$$\sigma = 4e^2\int\frac{\tau v^2}{3h^2}\left(-\frac{\partial f_0}{\partial\varepsilon}\right)d\mathbf{k} = \\ = \frac{4e^2\tau\bar{v}^2}{3kT}\int\limits_{E_g}^{\infty} D(E)f(E)\,dE. \tag{25}$$

For the Maxwell–Boltzmann distribution, the identity

$$-\frac{\partial f_0}{\partial\varepsilon} = \frac{1}{kT}f_0, \quad f_0 = \exp\left(\frac{\mu-\varepsilon}{kT}\right),$$

holds, and the electric conductivity is approximated on screening length scale by

$$\sigma = \frac{4e^2}{3\pi h^2}\tau kT\exp\left(-\frac{E_g}{2kT}\right). \tag{26}$$

The electric conductance behavior of graphene-based superlattice structures is illustrated in Figs. 3 and 4.

3.3. Thermionic current

At $T = 0$ K, electrons take the minimum-energy configuration. The electrons in the donors fall into the acceptor levels until the acceptors are all filled; in this configuration, the Fermi level must lie at the donor level:

$$\mu(0) = \frac{1}{2}E_g - E_d.$$

At sufficiently high temperatures, the electrons in the filled band can be excited to the conduction band. When the density of holes in the filled band and the density of electrons in the conduction band become much larger than the number of donors and acceptors, the effects of donors and acceptors can be neglected, and the sample shows characteristics similar to those of

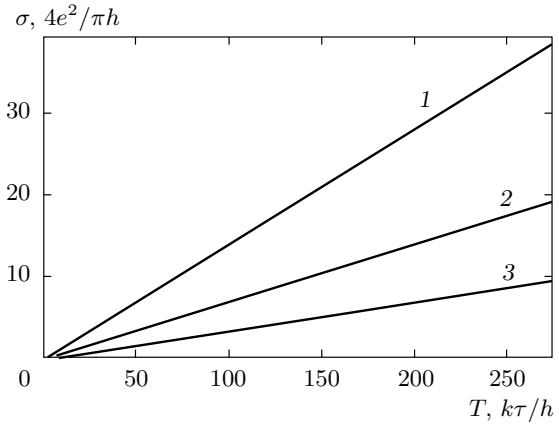

Fig. 3. The electric conductance behavior of the graphene-based superlattice structure shows enhanced mobilities at increased temperature. Evenly increasing the energy gap to the thermal energy ($E_g/kT \approx 7$, $E_g/kT \approx 14$, and $E_g/kT \approx 28$) shows a tendency to steady tunable electrical control and optical confinement on a length scale greater than the screening one

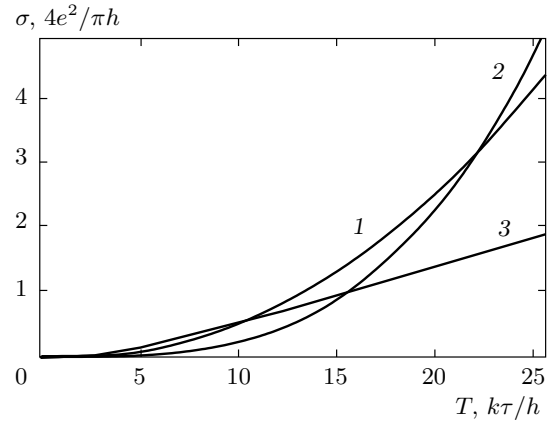

Fig. 4. Electric conductance behavior (power-law dependence on temperature) for intrinsic undoped graphene/GaAs/graphene (T^2-like behavior, *2*), undoped GaAs ($T^{3/2}$-like behavior, *1*) and the graphene-based modulation-doped superlattice structure InAs/graphene/GaAs/graphene/GaSb (T-like behavior, *3*). The undoped sample exhibits a relatively high conductance, unlike the doped one, which is more steady and less sensitive to the temperature, which is more valuable for tunable wide-band gap quantum devices

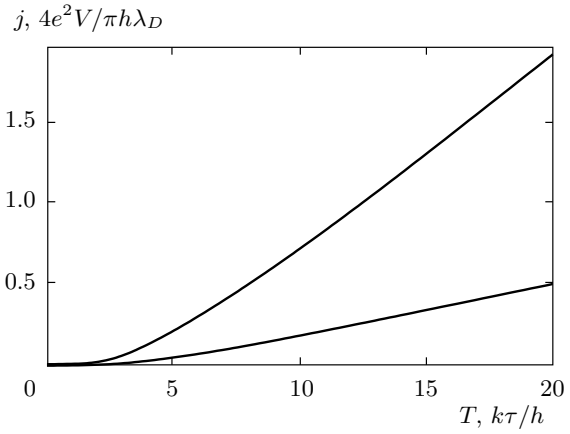

Fig. 5. The thermionic current density for different electrostatic potentials (the upper for (19) and the lower for (14)) fixed on the screening length scale shows a temperature dependence

an intrinsic semiconductor. In this case, the Fermi level is in the middle of the energy gap E_g and $\mu(\infty) = 0$. At the temperatures between these extreme cases ($T = 0$ and $T = \infty$), μ has a value between those given above. Summarizing, we can say that the behavior of μ is as follows: at $T = 0$ K, μ coincides with the donor level. It increases with the temperature and then approaches the middle of the gap between the conduction band and the filled band. This is not exact, but is sufficient for a qualitative discussion on the screening length scale.

At a finite temperature, electrons having higher energies than the work function $W = eV$ at the upper tail of the Fermi distribution can escape from the graphene surface to the interior of the superlattice structure in the direction normal to the surface. When an appropriate potential difference is applied, it is possible to collect all of the electrons escaping from the metal (graphene). For a graphene-based modulation-doped superlattice structure, the electric current density that occurs without any fluctuations in equilibrium can be written as $\mathbf{j} = \sigma\mathbf{E}$, where $\mathbf{E}$ can be represented as $\mathbf{E} = V(\mathbf{x})/\mathbf{x}$. In Fig. 5, we illustrate the thermionic current density behavior, which was enhanced due to a more realistic intrinsic electrostatic potential in (19).

4. CONCLUSION

We investigated electric transport properties for graphene-based modulation-doped superlattice structures providing a qualitatively good description. We have shown that slightly doped superlattice structures based on graphene monolayers as a high-conductivity channels, in tuning to the point of intrinsic-type structures where carrier concentrations are relatively insensitive to heat, generate less noise when operated at high frequencies, avoiding scattering effects on the screening length scale. The thermionic current density behavior is enhanced due to a more realistic intrinsic electrostatic potential, which was calculated taking the effect of metallic (graphene) monolayers into account. The proposed structure might be of great use for new types of wide-band energy gap quantum devices.

The authors are greatly indebted to Prof. J. Kwo and Prof. M. Hong for the stimulating discussions and fruitful suggestions. We acknowledge support from the National Center for Theoretical Sciences in Taiwan.

REFERENCES

1. K. S. Novoselov, A. K. Geim, S. V. Morozov, D. Jiang, M. I. Katsnelson, I. V. Grigorieva, S. V. Dubonos, and A. A. Firsov, Nature **438**, 197 (2005).
2. Y. Zhang, Y.-W. Tan, H. L. Stormer, and P. Kim, Nature **438**, 201 (2005).
3. C. Hummel, F. Schwierz, A. Hanisch, and J. Pezoldt, Phys. Stat. Sol. B **247**, 903 (2010).
4. B. L. Huang and C. Y. Mou, EPL **88**, 68005 (2009).
5. L. A. Falkovsky, Phys. Rev. B **80**, 113413 (2009); L. A. Falkovsky, Zh. Eksp. Teor. Fiz. **137**, 361 (2010).
6. M. Topsakal, H. Sevincli, and S. Ciraci, Appl. Phys. Lett. **92**, 173118 (2008).
7. H. Sevincli, M. Topsakal, E. Durgun, and S. Ciraci, Phys. Rev. B **77**, 195434 (2008).
8. P. Y. Chang and H. H. Lin, Appl. Phys. Lett. **95**, 082104 (2009).
9. M. K. Li, S. J. Lee, and T. W. Kang, Current Appl. Phys. **9**, 769 (2009).
10. M. Titov, P. M. Ostrovsky, and I. V. Gornyi, Semicond. Sci. Technol. **25**, 034007 (2010).
11. M. Titov and C. W. J. Beenakker, Phys. Rev. B **74**, 041401(R) (2006).
12. D. Bolmatov and C. Y. Mou, Zh. Eksp. Teor. Fiz. **137**, 695 (2010); D. Bolmatov and C. Y. Mou, Physica B: Condens. Matter **405**, 2896 (2010).
13. D. L. Miller, K. D. Kubista, G. M. Rutter, M. Ruan, W. A. de Heer, P. N. First, and J. A. Stroscio, Science **324**, 5929 (2009).

14. Yu. E. Lozovik, S. P. Merkulova, and I. V. Ovchinnikov, Phys. Lett. A **282**, 407 (2001); Yu. E. Lozovik and A. A. Sokolik, Phys. Lett. A **374**, 326 (2009).

15. M. Litinskaya and V. M. Agranovich, J. Phys.: Condens. Matter **21**, 415301 (2009).

16. J. Pomplun, S. Burger, F. Schmidt, A. Schliwa, D. Bimberg, A. Pietrzak, H. Wenzel, and G. Erbert, Phys. Stat. Sol. B **247**, 846 (2010).

17. M. Hong, J. Kwo, A. R. Kortan, J. P. Mannaerts, and A. M. Sergent, Science **283**, 1897 (1999).

18. M. Esmailpour, A. Esmailpour, R. Asgari, M. Elahi, and M. R. R. Tabar, Sol. Stat. Comm. **150**, 655 (2010).

19. M. Mucha-Kruczynski, E. McCann, and V. I. Fal'ko, Semicond. Sci. Technol. **25**, 033001 (2010).

20. X. Wang, Y. Ezzahri, J. Christofferson, and A. Shakouri, J. Phys. D: Appl. Phys. **42**, 075101 (2009).

21. S. Das Sarma and D. W. Wang, Phys. Rev. Lett. **83**, 816 (1999); D. W. Wang, A. J. Millis, and S. Das Sarma, Phys. Rev. Lett. **85**, 4570 (2000).

22. C. H. Shih, and C. C. Lin, Semicond. Sci. Technol. **25**, 065003 (2010).

23. L. K. Chu, W. C. Lee, M. L. Huang, Y. H. Chang, L. T. Tung, C. C. Chang, Y. J. Lee, J. Kwo, and M. Hong, J. Crystal Growth **311**, 2195 (2009).

24. K. Trachenko and M. T. Dove, arXiv:0805.1392v1.

25. P. Cisell, R. Zhang, Z. Wang, C. T. Reynolds, M. Baxendale, and T. Peijs, Eur. Polymer J. **45**, 2741 (2009).

26. H. Sevinli, M. Topsakal, and S. Ciraci, Phys. Rev. B **78**, 245402 (2008).

27. N. Abedpour, A. Esmailpour, R. Asgari, and M. R. R. Tabar, Phys. Rev. B **79**, 165412 (2009).

28. L. A. Chernozatonskii and P. B. Sorokin, Phys. Stat. Sol. B **245**, 2086 (2008); L. A. Chernozatonskii and P. B. Sorokin, J. Phys. Chem. C 114(7), 3225 (2010).

29. Yu-Xian Li, J. Phys.: Condens. Matter **22**, 015302 (2010).

30. Z. P. Niu, F. X. Li, B. G. Wang, L. Sheng, and D. Y. Xing, Eur. Phys. J. B **66**, 245 (2008).

31. T. Ouyang, Y. P. Chen, K. K. Yang, and J. X. Zhong, EPL **88**, 28002 (2009).

32. A. K. M. Newaz, Y. Wang, J. Wu, S. A. Solin, V. R. Kavasseri, I. S. Ahmad, and I. Adesida, Phys. Rev. B **79**, 195308 (2009).

33. S. Saito and A. Zettl, *Carbon Nanotubes: Quantum Cylinders of Graphene*, Elsevier, Oxford (2008).

34. B. Borca, S. Barja, M. Garnica, J. J. Hinarejos, A. L. V. Parga, R. Miranda, and F. Guinea, Semicond. Sci. Technol. **25**, 034001 (2010).

35. A. Nduwimana and Xiao-Qian Wang, Nano Lett. **9**(1), 283 (2009).

36. Y. P. Bliokh, V. Freilikher, S. Savel'ev, and F. Nori, Phys. Rev. B **79**, 075123 (2009).